Generation of Turning Motion for Tracked Vehicles Using Reaction Force of Stairs' Handrail

Yuto Ohashi, Shotaro Kojima, Kazunori Ohno, Yoshito Okada, Ryunosuke Hamada, Takahiro Suzuki and Satoshi Tadokoro

Abstract Inspections by mobile robots are required in chemical and steel plants. The robots are required to ascend and descend stairs because equipment components are installed on different-level floors. This paper proposes turning motion for tracked vehicles on stairs. A characteristic of the proposed turning motion is that it is generated using the reaction force from the safety wall of the stairs' handrail. The safety wall is commonly used in plants because it prevents objects from dropping down and damaging equipments. Proper turning motion is generated based on the motion model of the tracked vehicle. Experimental results show that the proposed turning motion can change the heading direction on the stairs. In addition, the proposed turning motion enables the vehicle to run with less slippage, as compared to other turning motions. The proposed method can reduce slippage by 88% while climbing up the stairs and by 44% while climbing down the stairs. The proposed method is more effective on the upward stairs than on the downward stairs. An autonomous turning motion control is implemented on the tracked vehicle, and it is evaluated on the upward stairs.

1 Introduction

Inspection using robot technologies is required to prevent accidents caused by equipment issues or deterioration in chemical and steel plants. It is considerably risky for human workers to inspect dangerous equipment components, such as blast furnace, during operation. The use of robot technologies can reduce the risk involved in the inspection of equipment during operation.

Tracked vehicles, which can climb up and down on stairs, are suitable for inspection because equipment components are installed on different-level floors. Therefore, we propose an inspection method using a tracked vehicle with sub-tracks, which is shown in Fig. 1 [1]. This vehicle can climb up and down on stairs. Instead of human workers, the vehicle can inspect equipments on different-level floors.

Y. Ohashi (✉) · S. Kojima · K. Ohno · Y. Okada · R. Hamada · T. Suzuki · S. Tadokoro
Tohoku University, Sendai, Miyagi 9800845, Japan
e-mail: ohashi.yuto@rm.is.tohoku.ac.jp

M. Hutter and R. Siegwart (eds.), *Field and Service Robotics*, Springer Proceedings in Advanced Robotics 5, https://doi.org/10.1007/978-3-319-67361-5_5

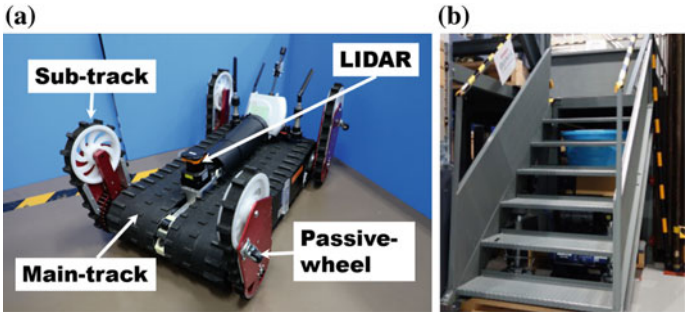

Fig. 1 Tracked vehicle "Quince" (**a**) and target stairs with safety walls (**b**)

An important function of tracked vehicles is to change the heading direction on the stairs. A track is a mechanism in which slippage occurs in principle on the ground and stairs. During the climbing up/down motion on the stairs, the heading direction changes because of slippage and gravity. Therefore, it is necessary to adjust the heading direction to the upward/downward direction on the stairs.

This paper proposes turning motion using the reaction force from the safety wall of the stairs' handrail, which prevents objects from dropping down. This is a new approach for changing the heading direction on the stairs. A characteristic of the proposed method is to generate the turning motion using the turning moment caused by the reaction force from the safety wall of the stairs' handrail. In general, tracked vehicles change heading directions using the difference between the velocities of the left and right tracks. The proposed method generates turning motion using the turning moment caused by the reaction force, in addition to the velocity difference. Experimental results show that the proposed method can reduce slippage on stairs, as compared to the turning motion based on the velocity difference.

The remaining part of the paper is organized as follows: Related works are explained in Sect. 2. The turning motion using the reaction force is proposed in Sect. 3. Proper velocity is derived from kinematics constraints. The proposed method is evaluated on the upward and downward stairs, and the results are provided in Sect. 4. The results show that the proposed method is effective on the upward stairs. Autonomous turning motion control is implemented on the tracked vehicle, and its evaluation on the upward stairs is described in Sect. 5. The paper is concluded in Sect. 6.

2 Related Works

Collisions with obstacles and the environment prevents proper motion of mobile robots because the reaction force caused the collision can damage the robot. Therefore, collision avoidance is an important research topic in the case of mobile robots. Several studies have been conducted on collision avoidance [2–6]. We consider that

the reaction force can be used to control motion. In this paper, the tracked vehicle does not prevent collision and positively uses the reaction force to change the heading direction on the stairs.

Motion control based on the reaction force is an important research topic in the case of mobile robots. Compliance control is a widely used technique. Compliance control enabled mobile robots or robotics arms can reduce the reaction force caused by a collision and move along the surface of objects or an environment [7–9]. Rude proposed a compliance control method using mechanical dampers and springs [10]. The proposed method could change the heading direction of mobile robots using the reaction force caused by collisions in a clutter environment. However, compliance control cannot move a vehicle in the appropriate direction. The purpose of compliance control is to reduce the reaction force. The motion generated using compliance control does not ensure that a mobile robot will face the target direction. This paper proposes turning motion using the reaction force. A kinematic model is used to determine the proper motion.

The reaction force from walls prevents mobile robots from generating proper turning motion. Kojima et al. proposed a control method to prevent this problem [11]. The study suggests that the proper control rule enables to generates turning motion by using the reaction force. Additionally, the method did not require direct measurement of the reaction force, and it generated proper turning motion. The approach proposed in this paper is based on the same perspective as that of the previously mentioned research, and it can generate proper turning motion on the stairs.

3 Turning Motion Using Reaction Force

This paper proposes a new method for generating turning motion on the stairs. The proposed method uses the difference between the speeds of left and right tracks and the reaction force to generate turning motion. In general, turning motion is generated using the difference between the speeds of the left and right tracks. Turning moment is generated using only the difference between these speeds. The turning moment generated using the reaction force is larger than that generated using the difference between the speeds of the left and right tracks. We consider that a combination of the speed difference and the reaction force can generate an even larger turning moment.

The safety wall of the stairs' handrail is used to generate the reaction force. The safety wall is commonly used in chemical and steel plants because it prevents objects from dropping down and damaging equipment.

Passive wheels are attached to the side of the sub-tracks, which is shown in Figs. 1a and 2. These wheels can reduce the friction force between the safety wall and wheels. Without passive wheels, the friction force prevents the tracked vehicle from turning on the stairs. In addition, the use of passive wheels reduces the damage to the safety wall and tracked vehicle.

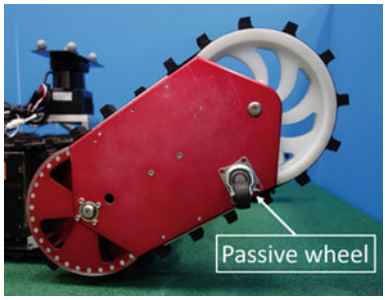

Fig. 2 Passive wheel attached to sub-track

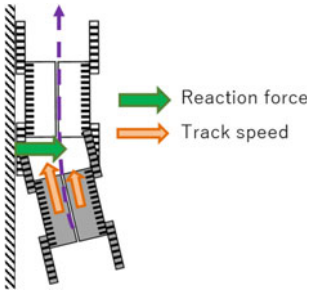

Fig. 3 Proposed turning motion and and its trajectory for the tracked vehicle on stairs

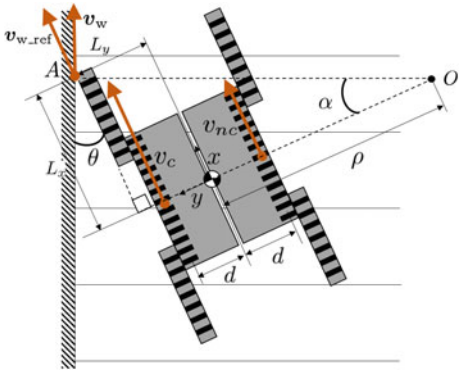

Fig. 4 Kinematic model of the tracked vehicle that contacts the stairs' handrail

The tracked vehicle moves as shown in Fig. 3; it moves and turns along the safety wall using the reaction force. To generate this turning motion, we need to consider how to derive the proper torque and speed of the left and right tracks. This paper proposes a speed control method based on the kinematic model of the turning motion of the tracked vehicle shown in Fig. 4. A coordinate frame is attached to the center of the vehicle body, in which the x-axis faces the vehicle's front and the y-axis faces its left. The turning center is O. Table 1 defines the parameters of this kinematic model. It is possible to derive the velocity condition using the kinematic model even if contact state varies.

Table 1 Parameters of the kinematic model

v_c	Peripheral velocity of contact side track
v_{nc}	Peripheral velocity of non-contact side track
$\boldsymbol{v}_w$	Actual velocity vector of contact point with the wall
$\boldsymbol{v}_{w\_ref}$	Commanded velocity vector of contact point with the wall
$2d$	Tread
L_x	Distance between center of gravity and contact point on x-axis
L_y	Distance between center of gravity and contact point on y-axis
θ	Angle between wall and robot
α	Angle between line segment from contact point to axis of rotation and the line segment from axis of rotation to center of gravity
ρ	Turning radius

To generate the reaction force, it is necessary for the tracked vehicle to move toward the wall direction that is represented by velocity $\boldsymbol{v}_{w\_ref}$ at contact point A in Fig. 4. This is the commanded velocity at contact point A. When the tracked vehicle moves along the wall because of the reaction force, the actual velocity, $\boldsymbol{v}_w$, is parallel to the safety wall at point A. In this case, the center of the turning motion exists on the line that is perpendicular to the wall at contact point A. When the tracked vehicle does not contact the wall, the center of the turning motion does not exist on the line.

The condition under which the robot maintains contact with the wall is derived using the kinematic model as

$$\theta + (90^\circ - \alpha) \geq 90^\circ \tag{1}$$

Angle α is

$$\alpha = \arctan\left(\frac{L_x}{L_y + \rho}\right) \tag{2}$$

Based on Eqs. (1) and (2), the condition of contact with the wall is

$$\tan\theta \geq \frac{L_x}{L_y + \rho} \tag{3}$$

Velocity v and angular velocity ω are given by

$$v = \frac{v_c + v_{nc}}{2} \tag{4}$$

$$\omega = \frac{v_c - v_{nc}}{2d} \tag{5}$$

Therefore, turning radius ρ is

$$\rho = \frac{v}{\omega} = \frac{d\,(v_c + v_{nc})}{v_c - v_{nc}} \tag{6}$$

As the robot wishes to turn around turning center O clockwise, the following relationship is obtained:

$$v_c > v_{nc} > 0 \tag{7}$$

The condition under which the robot maintains contact with the wall can be obtained using Eqs. (3), (6), and (7) as follows:

$$v_{nc} \geq \left(\frac{L_x - (d + L_y) \tan\theta}{L_x + (d - L_y) \tan\theta} \right) v_c \tag{8}$$

By moving such that this condition is satisfied, it is possible to perform a turn along the wall while continuously obtaining the moment due to the wall reaction force, as shown in Fig. 3.

4 Evaluation of Turning Motion Generated Using Reaction Force from Safety Wall of Stairs' Handrail

4.1 Evaluation Method

The following three turning methods are implemented on the tracked vehicle and compared on the stairs:

A: **Reaction force based turning motion (reaction force)** The tracked vehicle moves forward, without turning motion. The heading direction is changed by the reaction force caused by the forward motion.

B: **Turning motion based on differential between left and right track speeds (differential)** The tracked vehicle turns when it contacts the wall. The turning motion is generated using only the difference between the speeds of the left and right tracks.

C: **Proposed turning motion (reaction force + differential)** The tracked vehicle turns when it contacts the wall. The turning motion is generated using the reaction

force from the wall and the difference between the speeds of the left and right tracks.

The same initial conditions and pose were used for these evaluations. The vehicle started the motion upon contact with the wall, and its angle, θ, was 15°. The vehicle climbed the stairs, which were at an inclination of 40°, as shown in Fig. 1b. Typically, the tracked vehicle stretches the front and rear sub-tracks when it climbs the stairs for stabilizing itself. In motions B and C, the robot started turning from the beginning, and after completing the turn, it proceeded straight at the rotational velocity of the main tracks' motor, which was 2000 rpm. Each running test was performed three times.

The rotational speed of the motor at the contact side was set at 2000 rpm. The velocity of the track at the contact side was obtained using the gear ratio from the motor to the output shaft, n, and the pulley diameter, D, using the following equation:

$$v_{\mathrm{c}} = 2000\, nD \ [\mathrm{m/s}]. \tag{9}$$

The velocity of the track at the non-contact side, v_{nc}, can be obtained from the Eqs. (8) and (9). Therefore, the track velocity on the non-contact side was determined such that it satisfied. Here, $2d = 0.37$ m, $L_{\mathrm{x}} = 0.41$ m, and $L_{\mathrm{y}} = 0.28$ m. Therefore, v_{nc} is derived as follows:

$$v_{\mathrm{nc}} \geq 1485\, nD \ [\mathrm{m/s}]. \tag{10}$$

The velocity which is used in Eqs. (4)–(8) can be used with the actual track velocity or the approximated value of the commanded track velocity. Here, we use the command velocity. Table 2 shows the track speeds at the contact and non-contact sides for each type of motion. The rotational speed of the motor at the non-contact side was derived using Eq. (10) for motions B and C. v_{nc} of motion C is 1500 nD, which satisfies the condition of the robot maintaining contact with the wall as shown in Eq. (10). Turning time, which is the time required by the robot to directly face the stairs, was determined empirically based on the result of a preliminary experiment.

The above three motions are evaluated using movie and motion capture data. Turning angular velocity is calculated using the motion capture data during the turning motion. For motion A, turning time is the time required to climb the first step. For motions B and C, turning times are provided in Table 2. In addition, moving speed and slippage of robot are evaluated using the motion capture data because slippage is an important factor for turning motion on the stairs.

Slippage is evaluated using a vertical velocity ratio as shown in Eq. (11).

$$Vertical\ velocity\ ratio = \left| \frac{v_{\mathrm{z\_ref}} - v_{\mathrm{z}}}{v_{\mathrm{z\_ref}}} \right|. \tag{11}$$

where v_{z} is the current vertical velocity and v_{z}_ref is the commanded vertical velocity. If the vertical velocity ratio is larger than 1, it can be judged that slippage occurs in the z direction. This equation is determined in reference to slip ratio. Slip distance is

Table 2 Rotational speed and turning time

Motion	Rotational speed of contact side [rpm]	Rotational speed of non-contact side [rpm]	Turning time [s]
A: Reaction force	2000	2000	–
B: Differential	2000	1000	1.8
C: Reaction force + differential	2000	1500	2.0

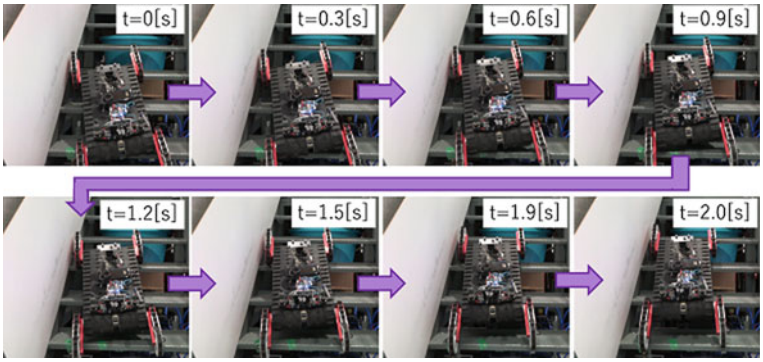

Fig. 5 Proposed turning motion, which uses reaction force from the wall while climbing

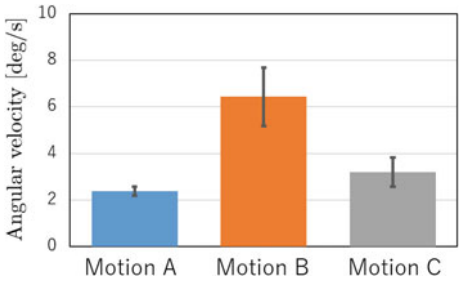

Fig. 6 Turning angular velocities while climbing; A: Reaction force, B: Differential, C: Reaction force + differential

derived by integrating the velocity in the vertical direction while slipping. The slip and the time required to run the stairs was evaluated as the time over which the vertical displacement changed by one step, which is at a height of 0.21 m from the start of trial. These two parameters were evaluated using tracking software (Tracker3.3, Vicon), based on with the images obtained using a motion capture camera (VANTAGE V5, 5 million pixels, Vicon). The sampling frequency of the motion capture camera was 100 [Hz]. Motion capture is used only to evaluate the motions.

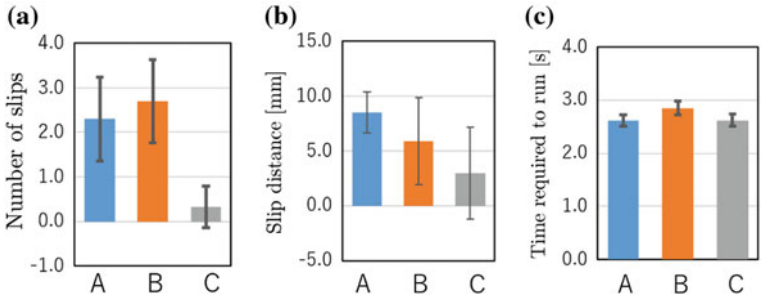

Fig. 7 Number of slips, and slip distance, and time required to run while climbing. A: Reaction force, B: Differential, C: Reaction force + differential

4.2 Evaluation of the Turning Motion on the Upward Stairs

Movie and motion capture data were recorded during the evaluations. The recorded movies showed that motions A, B, and C generated the turning motion on the stairs. Even though these behaviors were different, it was difficult to observe the difference in the movies. Figure 5 shows the turning motion generated by motion C (reaction force + differential).

Motion data were used to analyze the difference between these turning motions on the upward stairs. The angular velocity of each motion while commanding the turn is shown in Fig. 6. The figure shows that turning is the fastest in motion B at an angular velocity of 6.4°/s and the second fastest in proposed motion C at 3.2°/s. In motion A, turning is at 2.4°/s.

The number of slips, slip distance, and time required to run are shown in Fig. 7. It can be seen from Fig. 7a that the number of slips is 0.33 times for proposed motion C, which is the smallest value, 2.3 times for motion A, and 2.7 times for motion B. Figure 7b shows that the slip distance is 2.97 mm for proposed motion C, which is the smallest value, 5.90 mm for motion B, and 8.51 mm for motion A. It can be observed from Fig. 7c that the time required to run 2.74 s for motion A and proposed motion C, which is shorter than that for motion B, i.e., 2.96 s. Based on these results, proposed motion C (reaction force + difference) was determined to be the turning motion with the least slip and the fastest speed of climbing the stairs.

4.3 Evaluation of the Turning Motion on the Downward Stairs

The recorded movie and motion capture data were used to analyze the difference between the turning motions generated by motions A, B, and C on the downward stairs. Figure 8 shows the turning motion generated by motion C (reaction force +

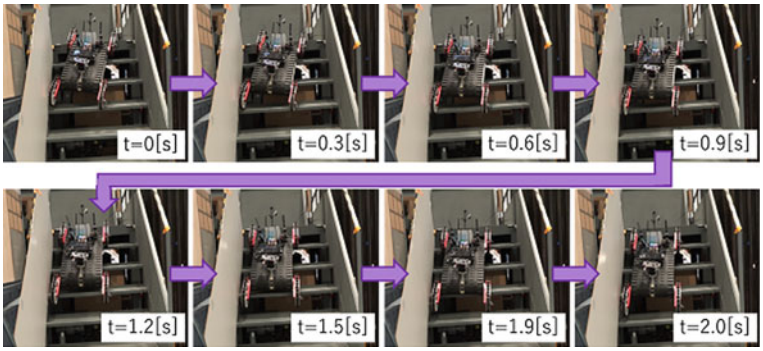

Fig. 8 Proposed turning motion, which uses reaction force from the wall while descending

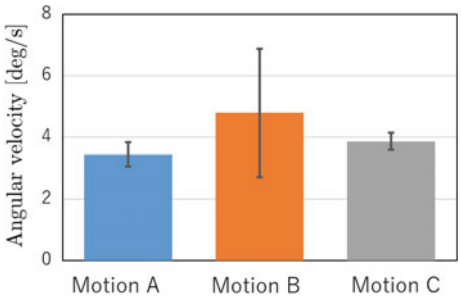

Fig. 9 Turning angular velocities while descending; A: Reaction force, B: Differential, C: Reaction force + differential

differential). The angular velocity of each motion while commanding the turn is shown in Fig. 9. The figure shows that the angular velocity is 4.8°/s for motion B, which is highest value, 3.9°/s for proposed motion C, which is the second highest value, and 3.4°/s for motion A.

The, number of slips, slip distance, and time required to run are shown in Fig. 10. It can be seen from Fig. 10a that the number of slips is 5 times for proposed motion C, which is the smallest value, 6 times for motion A, and 9 times for motion B. Figure 10b shows that slip distance is 38.9 mm for proposed motion C, which is the smallest value, 71.1 mm for motion A, and 82.7 mm for motion B. Figure 10c shows that the time required to run is 1.99 s for motion A, which is shorter than motion B and proposed motion C, i.e., 2.39 s. Based on these results, proposed motion C (reaction force + differential) was determined to be the turning motion with the least slip while descending.

4.4 Discussion

The results show that the proposed method (motion C: reaction force + differential) generated proper turning motion and reduced the number of slips and slip distance

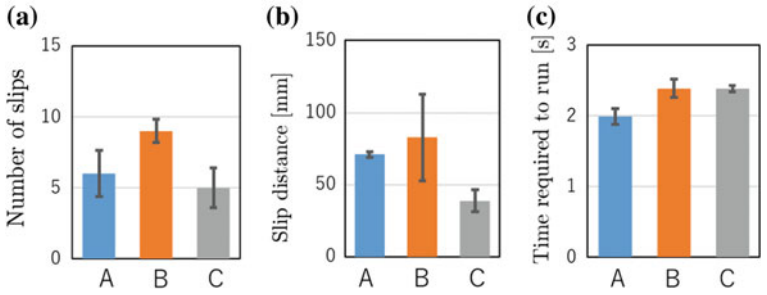

Fig. 10 Number of slips, slip distance, and time required to run while descending. A: Reaction force, B: Differential, C: Reaction force + differential

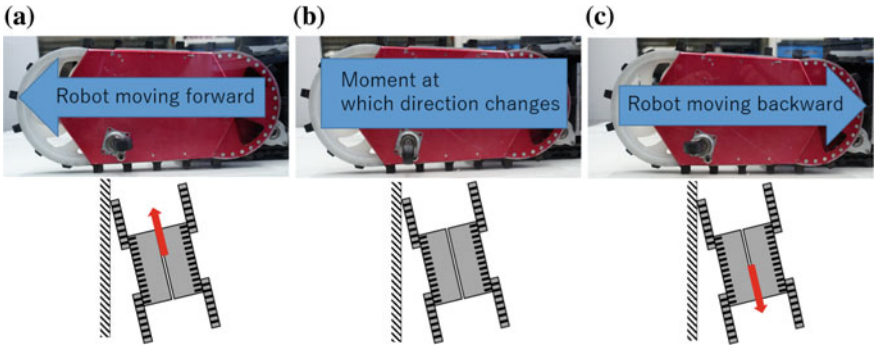

Fig. 11 Rotational characteristic of the caster: robot moving forward (**a**), moment at which direction of progression changes (**b**), robot moving backward (**c**)

while climbing up/down the stairs. A combination of reaction force and differential speed is a suitable solution for generating turning motion on the stairs.

There was considerable difference between the number of slips and total slip distance while climbing up and down the stairs. We analyzed the reason for this difference. We consider that the passive wheel attached to the sub-tracks causes this difference. The passive wheel consists of one wheel and one rotational axis, which is offset between the wheel and rotational axis. The rotational direction of the passive wheel changes depending on the motion of the tracked vehicle, as shown in Fig. 11. When the tracked vehicle slips while ascending, the direction of the wheel changes as Figs. 11a and b. At that instant, friction force is generated between the passive wheel and wall. This friction prevents the vehicle from slipping down on the stairs.

On contrary, when the tracked vehicle climbs down the stairs, the direction of the vehicle and slip is the same, and the direction of the passive wheel does not change. Therefore, friction force is not generated.

Based on these observations, it can be said that the passive wheel reduces the friction force between the sub-track and wall, and increases the friction during slippage when climbing up the stairs. This characteristic is considerably important for improving the turning motion when climbing up the stairs.

5 Autonomous Turning Motion on the Stiars

5.1 Implementation Method

To use the proposed motion for plant inspection or pilot assistance, turning motion is implemented on the tracked vehicle. To automate turning control, the control method requires the detection of contact and the measurement of the angle, θ, between the wall and the vehicle. The control flow, which decides velocity from detection of the contact and contact angle, θ, is shown in Algorithm 1.

Contact with the wall is detected using the roll angle of the main body and the electrical current value difference between the left and right main tracks' motors. It was experimentally determined that the current value of the main motor on the non-contact side increases and that on the contact side decreases upon contact with the wall during forward motion. Therefore, contact with the wall is detected when the current value difference is more than 4.5 A. This value is decided empirically. When running in a diagonal direction on the stairs, the roll angle of the robot is used to judge whether the robot is facing left or right with respect to the stairs (positive or negative roll angle). This can prevent the misjudgment of contact.

Algorithm 1 Decides velocity from detection of the contact and contact angle, θ.

loop
  $\{I_{\mathrm{L\_ave}}, I_{\mathrm{R\_ave}}\} \leftarrow$ Average of current value of {left, right} track motor for the past 5 times
  $\phi \leftarrow$ Roll angle of the robot from IMU
  $\theta_{\mathrm{ave}} \leftarrow$ Average of contact angle for the past 5 times which obtained from point cloud data
  if $(I_{\mathrm{L\_ave}} - I_{\mathrm{R\_ave}} < -I_{\mathrm{th}})$ **and** ϕ is negative **then** // Detect left side contact with the wall
    while $|\theta| > \theta_{\mathrm{th}}$ **do** // θ_{th} is threshold of contact angle
      Decide the right side motor speed using Eqs.(7) and (8)
    end while
  else if $(I_{\mathrm{L\_ave}} - I_{\mathrm{R\_ave}} > I_{th})$ **and** ϕ is positive **then** // Detect right side contact with the wall
    while $|\theta| > \theta_{\mathrm{th}}$ **do**
      Decide the right side motor speed using Eqs.(7) and (8)
    end while
  else
    Set the both left and right side motor speed to default
  end if
  Command rotational speed to motor
end loop

The contact angle is detected using a 2D LIDAR(HOKUYO: UTM-30LX) attached to top of the vehicle (Fig. 1a). The point cloud data on the wall are extracted

from scan data, and the wall is detected using liner approximation. To reduce false detection, the point cloud data that are located between 0.3 and 1.0 m from the vehicle are used for wall detection. The contact angle, θ, is obtained from the wall detected using the point cloud data and the heading direction of the vehicle. Then, proper track velocity is obtained from the Eqs. (7) and (8). The rotational speed of the motor at the contact side is set as 2000 rpm. The track velocity at the non-contact side can be obtained. In addition, when the contact angle is less than 5° or the wall is not detected, the velocity at the non-contact side is not updated using Eqs. (7) and (8). This can reduce the improper turning motion.

5.2 Evaluation Method

Autonomous turning control is evaluated based on the comparison between the following two methods:

Reaction force based turning motion The tracked vehicle moves forward, without turning motion. The heading direction is changed by the reaction force caused by the forward motion.
Proposed turning motion The tracked vehicle turns when it detects contact with the wall. Turning motion is generated using the reaction force from the wall and the difference between the speeds of the left and right tracks.

During the evaluation, the vehicle starts running without contact with the wall. The running distance is three steps, which is equal to a height of 0.63 m from the start. Other conditions are the same as those described in Sect. 4. A slip is counted when the slip distance exceeds approximately 2.4 mm, which is 10% of the interval of the grossers in the vertical direction of the stairs.

5.3 Evaluation Result

Figure 12 shows the images of the motion generated by the proposed control method. The vehicle turns left using the reaction force from the wall. Figure 13 shows the rotational velocity of the motor at the third trial of the proposed control method. Figure 13 shows that the rotational velocity of the motor at the non-contact side automatically changes at 2.2 s. Turning motion is automatically generated by the proposed method based on the detection of contact and the contact angle.

Figure 14 shows the number of slips, slip distance, and time required to climb the stairs for both turning control methods. The proposed turning control method reduces slippage during autonomous control. The number of slips for the proposed method is 1.76 times smaller than that for the other control method (Fig. 14a). The slip distance for the proposed method is 2.31 times smaller than that for the other method

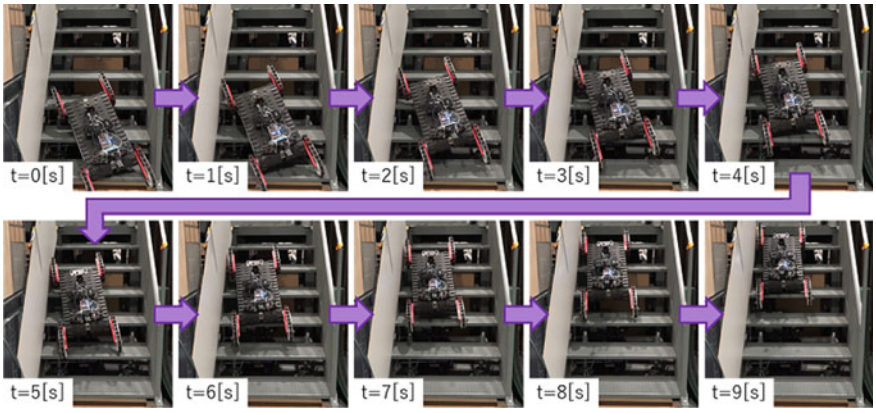

Fig. 12 Proposed automatic turning motion, which uses reaction force from the wall while climbing

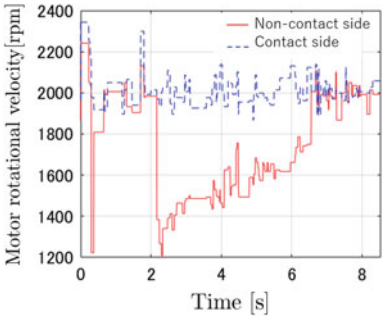

Fig. 13 Motor rotational velocity during the proposed turning motion which uses reaction force from the wall while climbing

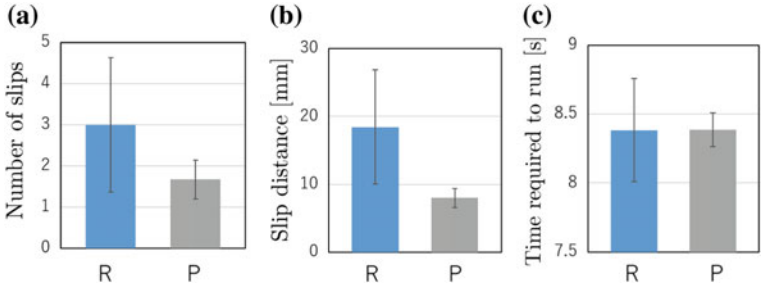

Fig. 14 Number of slips, slip distance, and time required to run while climbing. R: Reaction force based turning motion, P: Proposed turning motion

(Fig. 14b). The time required to climb the stairs is almost the same for both methods (Fig. 14c). These results show that proposed motion C (reaction force + differential) can generate proper turning motion and reduce slippage during the upward motion.

6 Conclusion

This paper proposed turning motion for a tracked vehicle on stairs. This turning motion was generated using the difference between the speeds of the left and right tracks and the reaction force from the safety wall. Movie and motion capture data were used to confirm that the proposed method generated proper turning motion on the stairs. In addition, the occurrence of slippage during the turning motion was evaluated. The results showed that the proposed method enables the vehicle to turn with less slippage compared to other methods (differential speed based, reaction force based). The proposed turning motion was more effective on the upward stairs than on the downward stairs. The passive-wheel caused less slippage during the upward motion because of the friction force between the passive-wheel and safety wall. Autonomous turning motion control was implemented on the tracked vehicle, and it was tested during the upward motion. It was observed that the proposed method enabled the vehicle to run with less slippage, as compared to the case in which turning motion was generated using only the reaction force from the wall.

Acknowledgements This research was supported by JST CREST Recognition, Summarization and Retrieval of Large-Scale Multimedia Data, Grant Number JPMJCR1403, Japan.

References

1. Rohmer, E., Yoshida, T., Ohno, K., et al.: Quince: a collaborative mobile robotic platform for rescue robots research and development. In: Proceedings of the 5th International Conference on Advanced Mechatronics: Toward Evolutionary Fusion of IT and Mechatronics, pp. 225–230 (2010)
2. Fox, D., Wolfram Burgard, W., Thrun, S.: The dynamic window approach to collision avoidance. IEEE Trans. Robot. Autom. **4**(1), 23–33 (1997)
3. Borenstein, J., Koren, Y.: Real-time obstacle avoidance for fast mobile robots. IEEE Trans. Syst. Man Cybern. **19**(5), 1179–1187 (1989)
4. Fox, D., Burgard, W., Thrun, S., et al.: A hybrid collision avoidance method for mobile robots. In: Proceedings of 1998 IEEE International Conference on Robotics and Automation vol. 2, pp. 1238–1243 (1998)
5. Fernández, J.L., Sanz, R., Benayas, J.A., et al.: Improving collision avoidance for mobile robots in partially known environments: the beam curvature method. Robot. Auton. Syst. **46**(4), 205–219 (2004)
6. Minguez, J., Montano, L.: Nearness diagram (ND) navigation: collision avoidance in troublesome scenarios. IEEE Trans. Robot. Autom. **20**(1), 45–59 (2004)
7. Mason, M.T.: Compliance and force control for computer controlled manipulators. IEEE Trans. Syst. Man Cybern. **11**(6), 418–432 (1981)

8. Salisbury, J.K.: Active stiffness control of a manipulator in Cartesian coordinates. In: Proceedings of 1980 19th IEEE Conference on Decision and Control including the Symposium on Adaptive Processes, vol. 19, pp. 95–100 (1980)
9. Kim, K.S., Kwok, A.S., Thomas, G.C., et al.: Fully omnidirectional compliance in mobile robots via drive-torque sensor feedback. In: Proceedings of 2014 IEEE/RSJ International Conference on Intelligent Robots and Systems, pp. 4757–4763 (2014)
10. Rude, M.: A flexible, shock-absorbing bumper system with touch-sensing capability for autonomous vehicles. In: Proceedings of IEEE/RSJ International Conference on Intelligent Robots and Systems, vol. 2, pp. 410–417 (1996)
11. Kojima, S., Ohno, K., Suzuki, T., et al.: Motion control of tracked vehicle based on contact force model. In: Proceedings of 2016 IEEE/RSJ International Conference on Intelligent Robots and Systems, pp. 1177–1183 (2016)